New Jersey Geological Survey
Open-File Report OFR 92-2

Field Guide to the Geology of Radon Hazard Areas in New Jersey

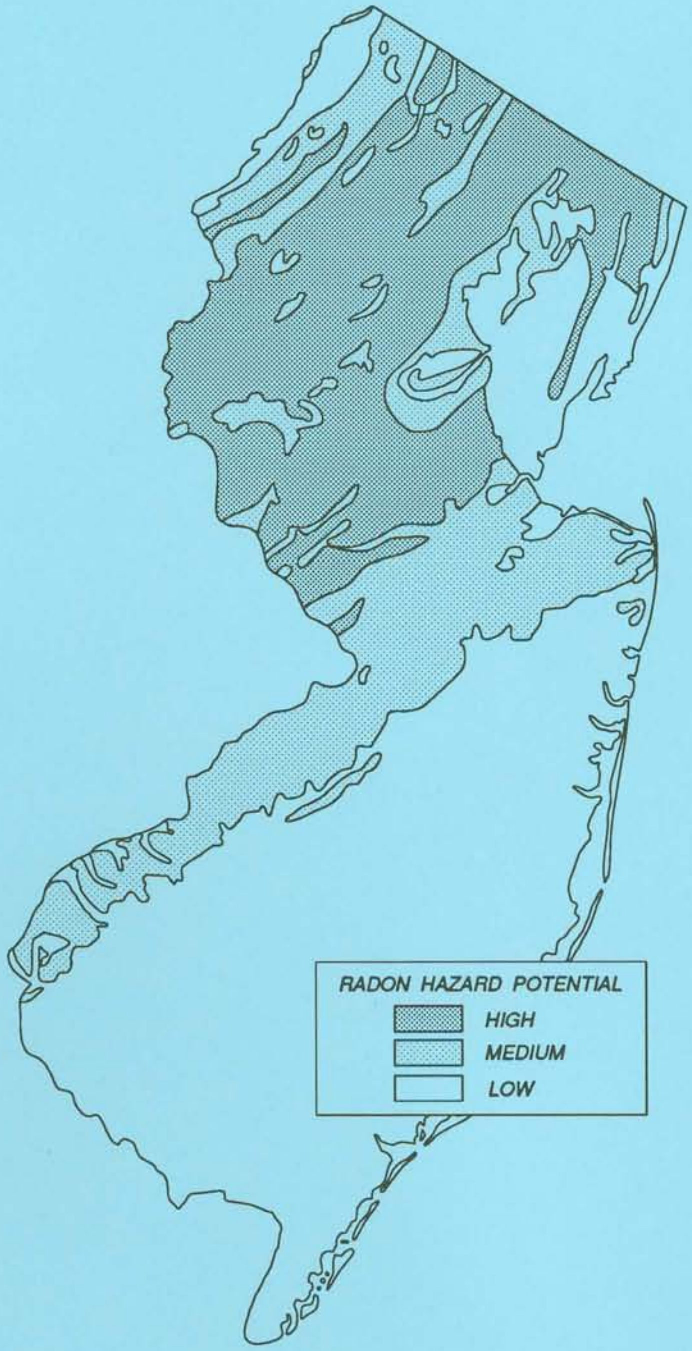

N.J. Department of Environmental Protection and Energy - Division of Science and Research

STATE OF NEW JERSEY
Jim Florio, *Governor*

Department of Environmental Protection and Energy
Scott Weiner, *Commissioner*

Policy and Planning
Richard V. Sinding, *Assistant Commissioner*

Division of Science and Research
Robert K. Tucker, Ph. D., *Director*

Geological Survey
Haig F. Kasabach, *State Geologist*

Cover Illustration: Radon hazard potential - simplified from the NJ DEPE "Statewide scientific study of radon, Summary report" (April 1988). The hazard rankings are based on the amount of radon available from radium in the rock or soil and the soil permeability (which allows radon to be transported into homes). The rankings were mapped according to the home indoor radon measurements referred to in the text (p. 1). Average radon levels for each rank are: high hazard: greater than 6.8 pCi/l; medium hazard: less than 6.8 pCi/l, greater than 4.6 pCi/l; low hazard: less than 2.1 pCi/l.

New Jersey Geological Survey
Open-File Report OFR 92-2

Field Guide to the Geology of Radon Hazard Areas in New Jersey

by

Karl Muessig, Hugh Houghton,
Donald Monteverde, Richard Volkert
New Jersey Geological Survey

This guide was prepared for a field excursion held in conjunction with the 24th annual meeting of the Northeastern Section, Geological Society of America (New Brunswick, New Jersey, March 23-25, 1989). It was printed in accordance with the Geological Survey's mission to disseminate educational and scientific information pertaining to the geology and mineral resources of New Jersey.

New Jersey Department of Environmental Protection and Energy
Division of Science and Research
Geological Survey
CN 427
Trenton, NJ 08625

1992

Printed on recycled paper

NEW JERSEY DEPARTMENT OF ENVIRONMENTAL PROTECTION AND ENERGY

The mission of the New Jersey Department of Environmental Protection and Energy is to conserve, protect, enhance, restore and manage our environment for present and future generations. We strive to prevent pollution; ensure the efficient use of safe, environmentally sound and reliable energy resources; provide opportunities for recreation and enjoyment of natural and historic resources; and promote a healthy and sustainable ecosystem.

New Jersey Geological Survey open-file reports are published by the New Jersey Geological Survey, CN-427, Trenton, NJ 08625. This report may be reproduced in whole or part provided that suitable reference to the source of the copied material is provided.

Additional copies of this and other reports may be obtained from:

Maps and Publications Sales Office
Bureau of Revenue
CN-417
Trenton, NJ 08625

A price list is available on request.

FIELD GUIDE TO THE GEOLOGY OF RADON HAZARD AREAS IN NEW JERSEY

INTRODUCTION

Radon gas, a product of radioactive decay of uranium-238 and thorium-232, has been identified as a cause of lung cancer from studies of uranium mine workers (Lundin and others, 1971; Whittemore and McMillan, 1983). The natural occurrence of radioactive radon gas in homes became widely publicized in the eastern United States following the discovery of extremely high levels in Boyertown, Pennsylvania, in December of 1984. In the spring of 1986, the first record of high radon levels in New Jersey was found throughout a subdivision of homes in Clinton, Hunterdon County. The Pennsylvania occurrence is associated with uranium-rich zones in the Middle Proterozoic crystalline rocks of the Reading Prong. In Clinton, the uranium-rich zone is in Paleozoic carbonate rocks adjacent to Middle Proterozoic rocks in the New Jersey Highlands. High radon levels in the Highlands are not surprising. The crystalline rocks of the Highlands have long been known to have radioactive mineral occurrences and were identified as a prime area of uranium resources by the National Uranium Resources Evaluation Program (NURE) of the 1970's (Baillieul and others, 1980; Popper and Martin, 1982). Elevated radon levels in carbonate units were unforeseen due to the absence of primary uraniferous minerals in the carbonate depositional environment. Preliminary studies of the Clinton area, which is underlain by carbonate rock, suggested that the uranium is associated with localized fault zones (Gabelman, 1956), but more study was needed of these rare occurrences to identify the nature of the secondary emplacement of the uranium.

Another surprise has been the widespread distribution of radon in the Piedmont Province. The NURE studies noted the potential for uranium mineralization in the Triassic-Jurassic rocks of the Newark Basin (Popper and Martin, 1982), which comprise most of the Piedmont Province in New Jersey. This potential was further highlighted in a paper by Turner-Peterson and others (1985) on the Lockatong and Stockton Formations. In developing a radiation protection program in New Jersey, nearly half of the effort has been expended in the Piedmont Province.

A clearer picture is now emerging of the geological controls on uranium distribution and the associated radon hazards in New Jersey. Regional geologic associations of uranium and radon developed from data collected by the New Jersey Geological Survey over the past two years are discussed below in the context of the field stops.

REGIONAL PATTERNS

Aerial Radiometric Data. As part of the NURE program, abundant aerial radiometric data were collected over New Jersey by the U.S. Department of Energy in the late 1970's. The original purpose of the program was to define potential uranium resources and identify areas for further exploration. Data collected during the geophysical surveys included gamma spectrometer counts of bismuth-214, thallium-208, and potassium-40. Bismuth-214 is a decay product within the uranium-238 decay series and can be used to estimate concentrations of uranium or radon, assuming radioactive equilibrium.

NURE flight-line data in New Jersey are spaced at three-mile intervals in the northern part of the State and six-mile intervals in the southern part of the State (fig. 1). In addition, a 1/4-mile-spaced survey was conducted over a large portion of the Highlands. As part of a statewide radon study, these data sets were reprocessed and contoured. Areas of anomalous bismuth-214 gamma activity, defined as exceeding 3 standard deviations above the mean of 2.4 ppm equivalent uranium, were highlighted as having the greatest source potential for elevated radon (fig. 2). Fifty anomalies exceeding 6 ppm were reflown to assure adequate delineation and to verify the reliability of the data.

Indoor Radon Survey. New Jersey is divided broadly into six geologic regions or provinces (fig. 2) for assessing regional trends in radiometric signatures. Geologic province is used here to denote regions that are characterized by similar geologic features such as age and lithology. In many but not all parts of the state, geologic provinces are coincident with the physiographic provinces.

Radon statistics for a 6,000-home survey are summarized in table 1 (page 4), along with the NURE equivalent uranium averages associated with the sampled homes. Provinces with mean equivalent uranium (eU) exceeding the statewide mean (2.4 ppm eU) have corresponding average radon levels exceeding 4 picocuries per liter (pCi/l). These provinces also contain most of the NURE anomalies which exceed the mean by three times the standard deviation (fig. 2). Conversely, provinces with average equivalent uranium

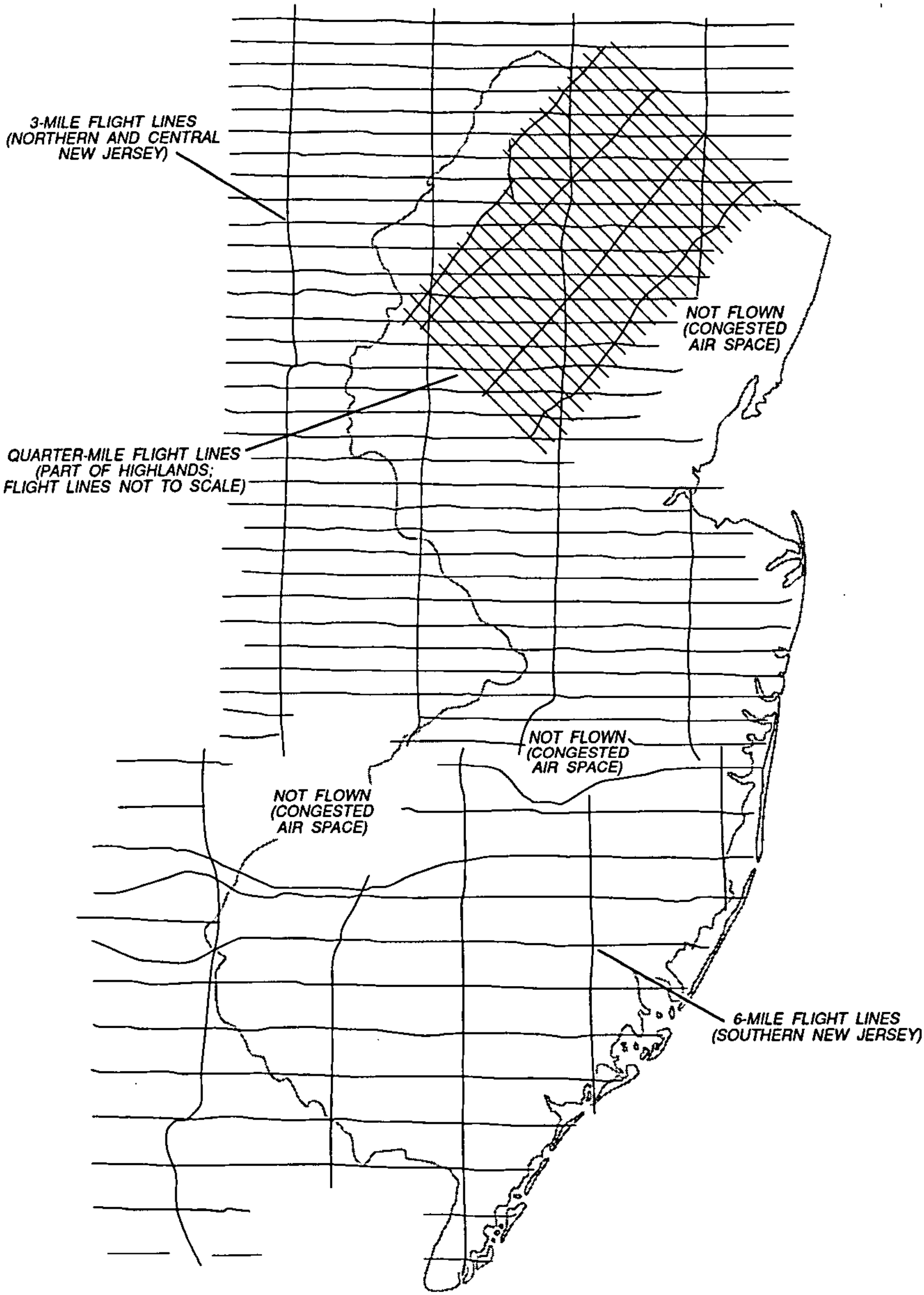

Figure 1. Flight lines for NURE aerial radiometric data in New Jersey.

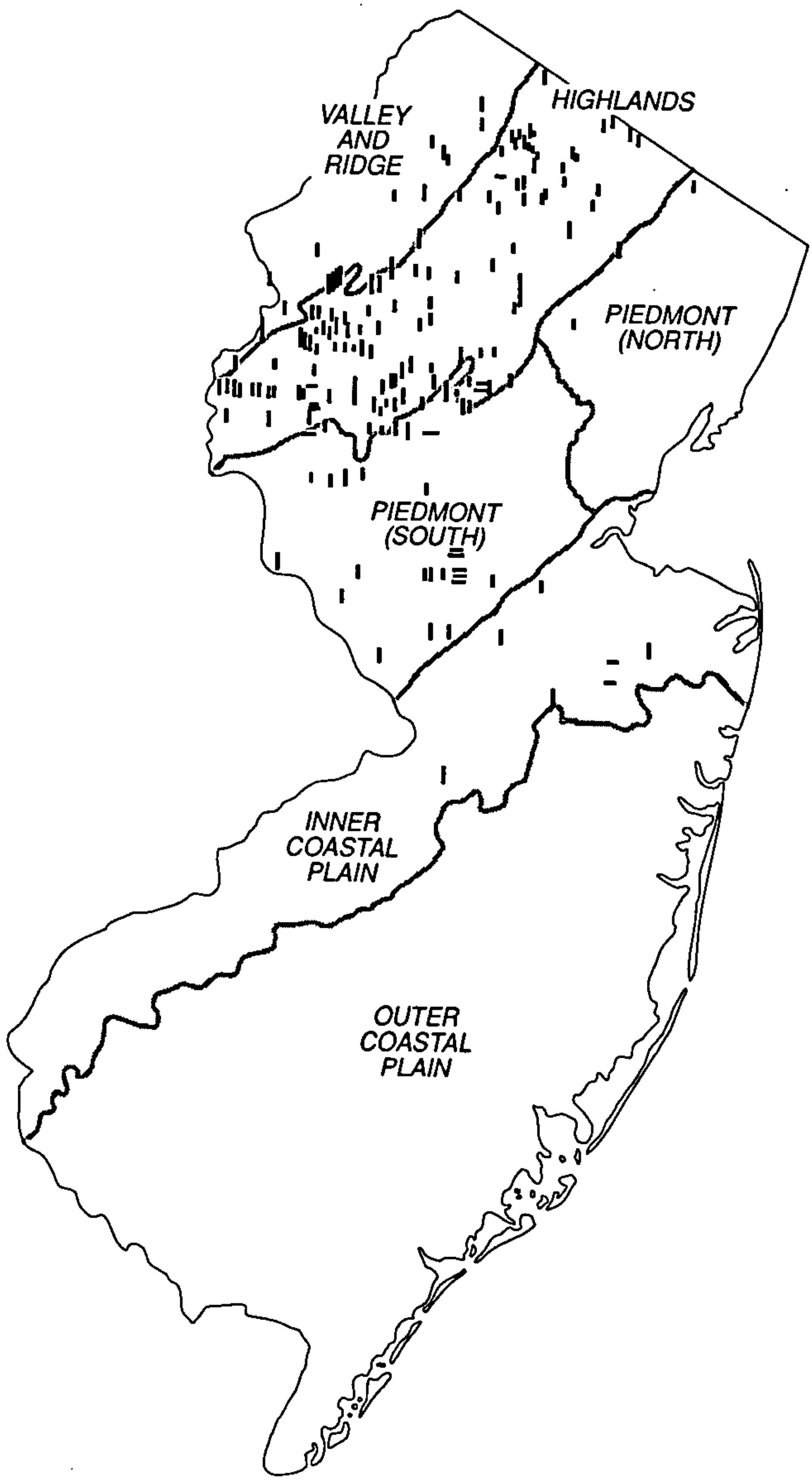

Figure 2. New Jersey geologic provinces and locations of NURE gamma anomalies greater than 3 standard deviations above the mean (2.4 ppm equivalent uranium).

TABLE 1.
INDOOR RADON STATISTICS AND NURE DATA FOR GEOLOGIC PROVINCES

Province/Number of Samples	Arithmetic Average	Geometric Mean*	Percent of Homes		NURE eU#
			≥4pCi/l	≥20pCi/l	
Valley & Ridge/684	7.6	4.5	57	8	2.5
Highlands (Reading Prong)/1,471	8.6	4.2	52	9	2.6
Piedmont (south)/1,610	4.9	2.5	32	4	2.7
Piedmont (north)/717	1.7	1.2	6	<1	2.1
Inner Coastal Plain/987	2.4	1.5	14	1	1.8
Outer Coastal Plain/258	1.4	1.0	5	<1	1.2
Statewide/5,727	5.2	2.4	33	5	2.4

* Average and mean indoor radon values in pCi/l are from Cahill and others (1988).
\# Average equivalent uranium (eU) in ppm.

values less than the statewide mean have corresponding radon averages less than 4 pCi/l and contain only a few NURE anomalies.

Cambrian and Ordovican sedimentary rocks in the Valley and Ridge Province and Middle Proterozoic crystalline rocks in the Highlands are the source of the most severe radon problems in the State. Radon levels in more than 50% of the homes in these provinces exceed 4 pCi/l.

The Piedmont Province comprises Triassic-Jurassic sedimentary and igneous rocks of the Newark Basin. There is a dramatic difference within the province north and south of the terminal moraine. The southern Piedmont has an elevated radiometric signature and moderate radon levels, with 32% of the homes exceeding 4 pCi/l. In contrast, the northern Piedmont has much lower radon and surficial radiometric levels, due partly to lithologic differences and also to a mitigating cover of glacial materials. Glacial cover is also a mitigating factor in the northern portions of the other high radon provinces discussed above.

The Coastal Plain Province, covering the southern part of New Jersey, comprises Cretaceous through Holocene sediments. Significant differences in radon and radioactivity are found between the Inner (northwestern) and Outer (southeastern) Coastal Plain. The Inner Coastal Plain consists mostly of restricted marine shelf sediments that contain abundant glauconite and are enriched in potassium and phosphorous. This area exhibits more elevated radon and aeroradiometric signatures (table 1) than the Outer Coastal Plain, where clean quartz sands dominate.

Confirmatory Data. The correlation of indoor radon levels with airborne radiometric data for nine anomalous areas is summarized in table 2. Five of the field trip stops are within anomalous areas. The nine areas have been ground checked by detailed geologic mapping, soil sampling, and ground radiometric traverses. The indoor radon data were collected under a state program of confirmatory monitoring in areas of elevated radon.

TABLE 2.
NURE VALUES FOR INDOOR RADON CLUSTERS

Location	NURE eU ppm*	Percent of Homes Monitored		
		>4pCi/l	>20pCi/l	>200pCi/l
Clinton, Hunterdon Co.	10	96	80	35
Montgomery, Somerset Co.	9	67	27	7
Ewing, Mercer Co.	8	78	40	5
Princeton, Mercer Co.	9	75	28	2
Bethlehem, Hunterdon Co.	7	75	35	11
Hampton, Hunterdon Co.	11	100	64	14
Bernardsville, Somerset Co.	9	87	45	9
Mansfield, Warren Co.	10	88	65	7
Washington, Morris Co.	10	87	57	13

* Peak value for the anomaly in the NURE data.

All localities studied are within or immediately adjacent to airborne radiometric anomalies which exceed 6 ppm eU. As might be expected, the spatial correlation of anomalies with elevated indoor radon is improved with more closely spaced data. Where 1/4-mile-spaced radiometric data exist (fig. 1), anomalies are detected on multiple flight lines and are coincident with clusters of elevated radon in homes in Bernardsville (Somerset County), Mansfield (Warren County), and Washington (Morris County). Anomalies detected in the three-mile data occur on one flight line, frequently are adjacent to areas where elevated radon has been detected, and occur along continuations of a geologic unit which causes home radon problems.

GEOLOGIC SOURCES OF RADON

Highlands
Radioactive elements occur naturally in a variety of Middle Proterozoic rocks in the New Jersey Highlands. The tendency is for radioactive minerals to be concentrated in potassium-rich granite, granite pegmatite, and alaskite. Some quartzofeldspathic gneisses are also elevated in radionuclides, especially those with a high K_2O-to-Na_2O ratio (Volkert, 1987). Brittle-fault zones with associated cataclastic textures frequently develop concentrations of radioactive minerals in these rock types. Brecciated and highly chloritized granites in these fault zones may contain allanite and secondary uranium minerals (Volkert, 1987; Volkert and others, 1989). Previous work has also shown uranium, thorium and rare earth mineralization occuring in association with some magnetite deposits (Klemic and others, 1959), and as thin layers within quartzofeldspathic gneisses near Chester (Markewicz, unpub. b; Volkert and others, 1990).

Paleozoic Sedimentary Rocks
Concentrations of uranium responsible for elevated radon in homes have been noted in four different environments: 1) quartzite of the Hardyston Formation, 2) dolomite of the Beekmantown Group, 3) slate of the Martinsburg Formation, and 4) shale and limestone of the Jutland sequence.

Uranium and thorium are concentrated in the Hardyston Formation in heavy mineral lag deposits at the basal unconformity with the Middle Proterozoic basement. The lower part of the unit has an immature arkosic composition and zircon and monazite are common minerals, especially in the basal meter of the quartzites. Widespread radon problems have not been encountered in association with the Hardyston quartzite due to the relative thinness of the uranium-rich lithology.

The second environment of uranium concentration is a unique occurrence in the Clinton area. Extremely high levels of radon in homes were discovered in Clinton in the spring of 1986. Subsequent studies by the New Jersey Geological Survey showed that the radioactivity is structurally controlled along fault and breccia zones. The breccia matrix contains up to 1,440 ppm uranium. In comparison, background levels are 1.4 ppm and 3.9 ppm uranium for the host dolomites and black shales respectively. Uranium-bearing minerals include apatite, and hydroxyapatite (Popper and Martin, 1982) and fluorapatite (M. Kaeding, written communication, 1988).

Preliminary studies of conodonts from the surrounding dolomites suggest that carbonate rocks in the area have undergone a hydrothermal event as recorded by their color index (J. Repetski, written communication 1988). Hydrothermal fluids may have been responsible for introducing uranium, thorium, rare earths, and phosphate as all are strongly correlated in chemical analyses of samples of radioactive dolomite from this area (M. Kaeding, written communication, 1988).

The third occurrence of uranium is in the Martinsburg Formation. The black slates of the lower Bushkill Member are slightly but uniformly elevated in uranium; however, no discrete uranium minerals have been found. This lithology is responsible for widespread elevated radon levels in the Valley and Ridge and in isolated areas within the Highlands.

Finally, several lithologies within the Jutland sequence are elevated in uranium. In the lower part of the sequence a black and brown shale section with interbedded limestone lenses has elevated radioactivity. The limestones are tightly folded and brecciated; fluorite is present in some of these rocks (Markewicz, unpub. a). Porous manganiferous layers and associated C soil horizons are found to contain 48 ppm uranium.

A second lithology found to be elevated in radioactivity occurs within varicolored shales of the Jutland sequence. Thin, tan laminae of friable shale may exhibit twice the radioactivity of surrounding units.

Triassic-Jurassic Newark Basin
Clusters of homes with elevated indoor radon are situated on Triassic rocks of the Newark Basin. All of these sites are located on uranium-enriched lithologies of the Lockatong and upper Stockton Formations. A sequence of strata near the base of the Lockatong Formation is associated with consistently high indoor radon levels. However, strata higher in the Lockatong Formation and within the upper part of the Stockton also cause local radon problems.

Uranium-thorium mineralization has been reported in two main modes of occurrence in the Newark Basin:

1) Scattered patchy or disseminated mineralization in sandstone of the Stockton Formation. Johnson and McLaughlin (1957) reported torbernite ($Cu(UO_2)_2(PO_4)_2$ 8-$12H_2O$) in a limonitic sandstone "vein" north of Stockton, New Jersey. McCauley (1961) reported disseminated metazeunerite ($Cu(UO_2)_2(AsO_4)_2 8H_2O$) and meta-autunite ($Ca(UO_2)_2(PO_4)_2 2$-$6H_2O$) in gray arkosic sandstone with brown iron-oxide specks from the Stockton Formation at Prallsville and Raven Rock, New Jersey. Turner-Peterson (1980) reported patchy uranium-enriching alteration of clay clasts in iron-oxide-stained gray Stockton sandstone from the Raven Rock area.

2) Disseminated, submicroscopic uranium-thorium minerals in beds of black to gray carbonaceous mudstone to claystone and gray fine sandstone to siltstone in lake-bed sequences of the Lockatong and Passaic Formations. Turner-Peterson and others (1985) discussed mineralization in lake beds of the upper Stockton and the Lockatong Formations and believe uranium is complexed with humic matter. Zapecza and Szabo (1987) reported radioactive gray to black mudstone in the lower Passaic Formation. No discrete mineral phases have been identified in the fine-grained lake bed occurrences. Autoradiographs of black mudstone typically show evenly distributed radioactive specks spaced a few millimeters apart, and commonly show radioactive concentrations in coarse-grained laminae.

The first mode of occurrence has only been reported from the Stockton Formation near the Delaware River. It is not known whether the Stockton sandstone occurrences are localized or widespread. Severe radon problems have been identified recently in association with arkosic sandstone facies in the Clinton area. Occurrences in Princeton may be localized along fault zones in the Stockton sandstone.

Uranium-thorium mineralization of the second type, in bedded lake-bottom, lake-margin, and playa deposits of the Lockatong and lower Passaic Formations, is abundant and widespread and has been identified as a source of regional radon anomalies.

Basin-fill sediments of the uppermost Stockton, the entire Lockatong, and the lower half of the Passaic Formations record cycles of dry basin flooding, lake filling, lake recession, and return to dry basin conditions. These climate-forced cycles, which are discussed at length by Van Houten (1962, 1964) and Olsen (1980, 1984), produced rhythmically-bedded sedimentary sequences mostly 3-10 m thick. Each cycle can be divided into three divisions (fig. 3). Division 1, which records the onset of more humid conditions, commonly consists of greenish-gray fine sandstone or laminated gray or tan siltstone with desiccation features, disrupted bedding, or pedogenic structures. Division 2 records the lake highstand and consists of lake-bottom beds of finely laminated to medium-bedded, fissile, carbonaceous claystone to siltstone, commonly calcareous and pyritic in some places. Division 3 records the recession of the main lake stage and return to more arid conditions, and usually consists of thick-bedded to massive, bioturbated siltstone with some desiccation-crack layers and evaporite-mineral casts.

Radioactivity anomalies occur in divisions 1 and 2 and in the lower part of division 3 with almost equal fre-

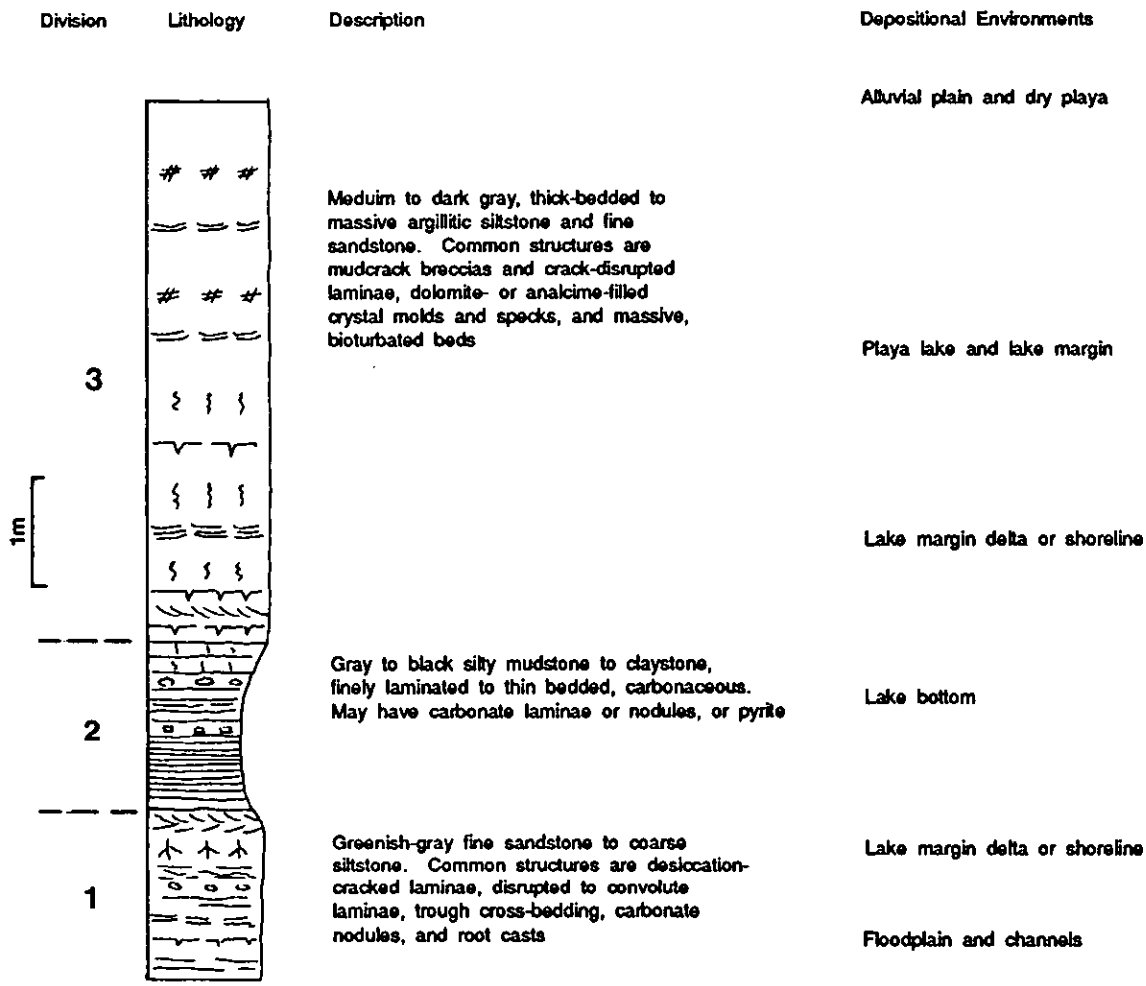

Figure 3. Diagrammatic section of a Lockatong lake cycle showing transgressive (1), lake high-stand (2), and regressive (3) divisions.

quency (table 3). Some anomalies have been followed along beds for more than 0.5 km and show little variation in intensity or thickness. Other beds, especially those with carbonate nodules, may vary in radioactivity by a factor of 2 to 3 over a distance of several meters.

Turner-Peterson and others (1985) reported uranium enrichment only in lake-bottom beds of division 2 and considered uranium occurrence to be controlled by the distribution of humic organic matter. However, several of the highest radioactivity anomalies are observed in lake-margin sandstones of divisions 1 and 3. Uranium/thorium mineralization appears to be controlled both by organic-matter content of lake-bottom mudstones and by porosity of sandstone beds adjacent to organic-rich layers. Additional petrographic and geochemical studies are needed to determine the exact mechanism and sequence of uranium mineralization.

TABLE 3.
MAXIMUM RADIOACTIVITY IN INDIVIDUAL LAKE-BED CYCLES, LISTED BY CYCLE DIVISION.

Cycle number	Maximum radioactivity (CPS)			Cycle number	Maximum radioactivity (CPS)		
	Div. 1	Div. 2	Div. 3		Div. 1	Div. 2	Div. 3
B2	350	150	120	B15	225	200	150
B3	235	360	1175	B16	480	190	190
B4	160	170	200	B17	550	190	150
B5	130	150	450	B18	140	175	475
B7	130	145	180	B19	125	135	130
B8	325	800	380	B20	180	130	110
B9	300	650	130	B21	375	225	150
B10	150	250	160	WC1	900	500	200
B11	160	250	450	RR2	250	1100	250
B12	180	225	250	WV1	200	190	400
B13	190	160	280	WV2	550	250	100
B14	150	190	180	WV3	90	90	95

Note: Cycle number prefixes correspond to localities: B = Byram cliffs on N.J. Rt. 29 (middle Lockatong Formation), WC = Warford Creek lake beds (lower Passaic Formation), RR = Raven Rock (lowermost Lockatong Formation), WV = Woodsville Road (lower Lockatong Formation). Radioactivity measured at Woodsville by hand-held scintillometer.

REFERENCES

Baillieul, T.A., Indelicato, G.J., and Penley, H.M., 1980, National uranium resource evaluation, Scranton quadrangle, Pennsylvania, New York and New Jersey; Bendix Field Engineering Corp. Report GJQ-003, *for* U.S. Dept. of Energy, Grand Junction, CO, 39 p.

Boynton, G.R., Pittillo, D.K., and Fandle, G.L., 1966, Natural gamma aeroradioactivity map of the Pittstown and part of the High Bridge quadrangles, New Jersey: U.S. Geological Survey Geophysical Investigation Map GP-573, scale 1:24,000.

Cahill, M.K., Nicholls, G.P., Ranney, C., and Rugg, M., 1988, Radon levels in New Jersey: Preliminary results of a statewide radon survey, *in* Proceedings of the 1988 Air Pollution Control Association, Dallas, Texas, 17 p.

Gabelman, J.W., 1956, Uranium deposits in limestone, *in* Page, L.R., Stocking, H.E., and Smith, H.B., eds., Contributions to the geology of uranium and thorium by the United States Geological Survey *and* Atomic Energy Commission *for* the United Nations International Conference on Peaceful Uses of Atomic Energy, Geneva, Switzerland, 1955: U.S. Geological Survey Professional Paper 300, p. 387-404.

Grauch, R.I., and Zarinski, K., 1976, Generalized descriptions of uranium-bearing veins, pegmatites, and disseminations in non-sedimentary rocks, eastern United States: U.S. Geological Survey Open-file Report 76-582, 114 p.

Hays, J.D., Imbrie, J., and Shackleton, N.J., 1976, Variations in the earth's orbit: Pacemaker of the Ice Ages: Science, v. 194, p. 1121-1132.

Henry, M.E., Kaeding, M.E., and Monteverde, Donald, 1991, Radon in soil gas and gamma-ray activity of rocks and soils at the Mulligan Quarry, Clinton, New Jersey, *in* Gundersen, L.C.S., and Warty, R.B., editors, Field studies of radon in rocks, soils and water, U.S. Geological Survey Bulletin 1971, p. 65-75.

Johnson, M.E., and McLaughlin, D.B., 1957, Triassic formations in the Delaware Valley, *in* Dorf, E., ed., Guidebook for field trips, Atlantic City meeting, Geological Society of America Annual Meeting, p. 31-67.

Klemic, H., Heyl, A.V., Taylor, A.R., and Stone, J., 1959, Radioactive rare-earth deposit at the Scrub Oaks Mine, Morris County, New Jersey: U.S. Geological Survey Bulletin 1082-B, 59 p.

Krauskopf, K.B., 1979, Introduction to geochemistry: New York, McGraw-Hill, 617 p.

Lundin, F.E., Wagoner, J.K., and Archer, V.E., 1971, Radon daughter exposure and respiratory cancer; quantitative and temporal aspects: Washington, D.C., U.S. Dept. of Health, National Institute for

Occupational Safety and Health, National Institute of Environmental Health Sciences Joint Monograph No. 1.

Markewicz, F.J., unpub. a, Geology of the High Bridge quadrangle: scale 1:24,000, on file in the office of the New Jersey Geological Survey [1967].

Markewicz, F.J., unpub. b, Chester monazite belt, on file in the office of the New Jersey Geological Survey [undated].

McCauley, J.F., 1961, Uranium in Pennsylvania: Pennsylvania Geological Survey Bulletin M43, 71 p.

New Jersey Department of Environmental Protection, 1989, Summary report, statewide scientific study of radon: *prepared by* Camp Dresser & McKee, Inc., Edison, N.J., variously paginated.

Olsen, P.E., 1980, The latest Triassic and early Jurassic formations of the Newark Basin (eastern North America, Newark Supergroup): New Jersey Academy of Sciences Bulletin, v. 25, p. 25-51.

— 1984, Periodicity of lake-level cycles in the Late Triassic Lockatong Formation of the Newark Basin, *in* Berger, A. L., ed., Milankovitch and Climate, NATO symposium, pt. 1, Dordrecht, Holland, D. Reidel, p. 129-146.

— 1986, A 40-million-year lake record of early Mesozoic orbital climatic forcing: Science, v. 234, p. 842-848.

Perissoratis, C., Brock, P.W.G., Brueckner, H.K., Drake, A.A., Jr., and Berry, W.B.N., 1979, The Taconides of western New Jersey: New evidence from the Jutland Klippe: Summary: Geological Society of America Bulletin, v. 90, part 1, p. 10-13.

Popper, G.H., and Martin, T.S., 1982, National uranium resource evaluation, Newark quadrangle, Pennsylvania and New Jersey: Bendix Field Engineering Corp. Report PGJ/F-123, *for* U.S. Dept. of Energy, Grand Junction, CO, 73 p.

Rejebian, V.A., Harris, A.G., and Huebner, J.S., 1987, Conodont color and textural alteration: an index to regional metamorphism, contact metamorphism, and hydrothermal alteration: Geological Society of America Bulletin, v. 99, p. 471-479.

Turner-Peterson, C.E., 1980, Sedimentology and uranium mineralization in the Triassic-Jurassic Newark Basin, Pennsylvania and New Jersey, *in* Turner-Peterson, C.E., ed., Uranium in Sedimentary Rocks: Application of the Facies Concept to Exploration, Society of Economic Paleontologists and Mineralogists, Short Course Notes, Denver, p. 149-175.

Turner-Peterson, C.E., Olsen, P.E., and Nuccio, V.F., 1985, Modes of uranium occurrence in black mudstones in the Newark Basin, New Jersey and Pennsylvania: U.S. Geological Survey Circular 946, p. 120-124.

Van Houten, F.B., 1962, Cyclic sedimentation and the origin of analcime-rich Upper Triassic Lockatong Formation, west-central New Jersey and adjacent Pennsylvania: American Journal of Science, v. 260, p. 561-576.

— 1964, Cyclic lacustrine sedimentation, upper Triassic Lockatong Formation, central New Jersey and adjacent Pennsylvania: Kansas Geological Survey Bulletin 169, p. 497-531.

Volkert, R.A., 1987, Geology, ground water occurrence, and ground water quality in the Middle Proterozoic rocks of the New Jersey Highlands: Proceedings of a short course on the Geology and Geohydrology of New Jersey, Part II, Geology and Geohydrology of the New Jersey Valley and Ridge, Highlands, and Lowlands Provinces, Rutgers University, New Brunswick, N.J., p. B1-B35.

Volkert, R.A., Monteverde, D.H., and Drake, A.A., Jr., 1989, Geologic map of the Stanhope quadrangle, Morris and Sussex Counties, New Jersey: U.S. Geological Survey, Geologic Quadrangle Map GQ-1671, scale 1:24,000.

Volkert, R.A., Markewicz, F.J., and Drake, A.A., Jr., 1990, Bedrock geologic map of the Chester quadrangle, Morris County, New Jersey: New Jersey Geological Survey, Geologic Map Series 90-1, scale 1:24,000.

Whittemore, A.S., and McMillan, A., 1983, Lung cancer mortality among U. S. uranium miners: A reappraisal: Journal of the National Cancer Institute, v. 71, p. 489-499.

Zapecza, O.S., and Szabo, Z., 1987, Source and distribution of natural radioactivity in ground water in the Newark Basin, New Jersey, *in* Graves, B., ed., Radon in ground water, proceedings of the NWWA conference: Chelsea, Michigan, Lewis Publishers, p. 47-68.

ROAD LOG AND FIELD STOP DESCRIPTIONS

Cumulative Mileage	Stop Mileage	Description
		Trip departs from Hyatt Regency Hotel, New Brunswick, take Easton Avenue north to I-287.
0.0	0.0	Get on I-287 northbound. Start mileage here.
10.4	10.4	Intersection of I-287 and I-78; take I-78 west.
20.4	10.0	Ridge on left is Cushetunk Mountain, underlain by Jurassic diabase. Ridges on right are underlain by Middle Proterozoic rocks.
20.9	0.5	We are crossing the trace of the Flemington fault, which juxtaposes Middle Proterozoic rocks on the footwall against Mesozoic rocks of the Newark Basin on the hanging wall.
22.9	2.0	Outcrops of Ordovician Rickenbach Formation on left.
23.3	0.4	Exit 17 - intersection of I-78 and Rt. 31. Bear right and follow signs for Rt. 31 north.
27.55	4.25	Outcrop of Middle Proterozoic pyroxene granite on right.
28.65	1.1	Turn right onto Sanitorium Road.
28.85	0.2	Straight ahead through stop sign; turn right just past RR bridge and proceed to quarry office.
29.05	0.2	STOP 1 - Lentine Aggregates quarry.

Stop 1 -

This quarry exposes a heterogeneous sequence of Middle Proterozoic rocks. From south to north these consist of pyroxene granite, pyroxene alaskite, sillimanite and garnet-bearing potassic feldspar gneiss, microperthite alaskite, and hornblende-pyroxene-quartz-plagioclase gneiss (fig. 4). Minor amounts of amphibolite occur as conformable interlayers in the gneiss and as inclusions in the granitic rocks.

Lithologic contacts are conformable in most places, although the microperthite alaskite locally crosscuts the foliation of the gneiss (fig. 5). The average foliation trend is N40°E within the quarry; foliation dips moderately to steeply to the southeast.

The majority of rock in the quarry is sheared and clearly shows both brittle deformation and greenschist-grade retrograde alteration (fig. 6, p. 10). The gross shearing appears to be subparallel to the foliation, but small, locally developed northwest-striking brittle deformation zones are common. Many of these shear planes are coated by chlorite or epidote. Films and fibrous growths of light-blue crocidolite occur as an alteration product on some shear planes in the quartzofeldspathic gneisses.

Levels of radioactivity were measured in the quarry with a portable scintillometer and recorded for each of the lithologies. The amphibolite, quartz-plagioclase gneiss, pyroxene alaskite, and pyroxene granite have uniformly low levels, ranging from about 120 to 200 counts per second (cps). Levels were locally elevated in the potassic feldspar gneiss and averaged about 170 to 250 cps, but range up to 800 cps. Quite expectedly, the most elevated levels were recorded in the microperthite alaskite, ranging from about 500 to 3,000 cps. The source of the elevated radioactivity appears to be thorite, thorogummite, fergusonite, and/or uranothorite (Markewicz, unpub. a).

Chemical analyses of various rock types from within the quarry are shown in table 4. An analysis of microperthite alaskite (sample HB-10) from just east of the quarry is shown also for comparison. It is readily apparent that the alaskites are enriched in U and Th over the rest of the lithologies in the quarry by up to several orders of magnitude. Possibly of greater significance for understanding the origin of the uranium is the fact that the comparatively undeformed alaskite (HB-10) contains higher values of U and Th than the brittly deformed alaskite (HB-6) from the quarry. The magnetite-rich cataclastic gneiss (HB-4) is some of the most highly sheared rock in the

TABLE 4.

MAJOR AND TRACE ELEMENT ANALYSES OF SOME REPRESENTATIVE LITHOLOGIES FROM LENTINE AGGREGATES QUARRY*

(WT%)	HB-1	HB-4	HB-5	HB-6	HB-10
SiO_2	69.70	49.20	73.30	72.80	71.40
Al_2O_3	13.80	12.90	11.30	14.00	14.50
Fe_2O_3[a]	3.68	22.70	5.31	1.21	1.16
MgO	0.32	0.94	0.18	0.21	0.53
CaO	1.35	1.53	0.29	0.65	1.38
Na_2O	4.75	3.61	2.70	4.09	2.81
K_2O	5.15	3.51	5.84	5.31	5.84
TiO_2	0.46	2.13	0.35	0.10	0.21
P_2O_5	0.10	0.65	0.02	0.03	0.07
MnO	0.09	0.23	0.09	0.03	0.02
LOI[b]	0.16	0.85	0.31	0.70	1.23
TOTAL	99.56	98.25	99.69	99.13	99.15
trace elements (ppm)					
Rb	120	120	180	140	190
Sr	90	40	<10	100	290
Ba	790	960	540	470	830
Zr	830	670	700	380	380
U	2.4	4.2	3.7	16.4	40.3
Th	0.8	10	2.2	130	650
La	38.2	106	34.4	65.4	350
Ce	93	218	52	73	450
Nd	63	97	26	24	119
Sm	10.8	19.1	3.7	2.9	11.4
Eu	4.0	6.1	2.3	2.2	1.3
Tb	2.2	2.9	0.6	<0.8	1.8
Yb	4.8	12.7	5.4	1.0	1.4
Lu	0.78	1.86	0.85	0.17	---
Y	80	120	70	<10	30

*Major and trace elements by XRF; rare earth elements by INAA. Analyses by XRAL Activation Services, Ann Arbor, Michigan.

a. Total iron as Fe_2O_3

b. Loss on ignition

HB-1 Pyroxene granite
HB-4 Magnetite-rich cataclasite
HB-5 Potassic feldspar gneiss
HB-6 Microperthite alaskite
HB-10 Microperthite alaskite from 2.5 mi. east-southeast of Stop 1

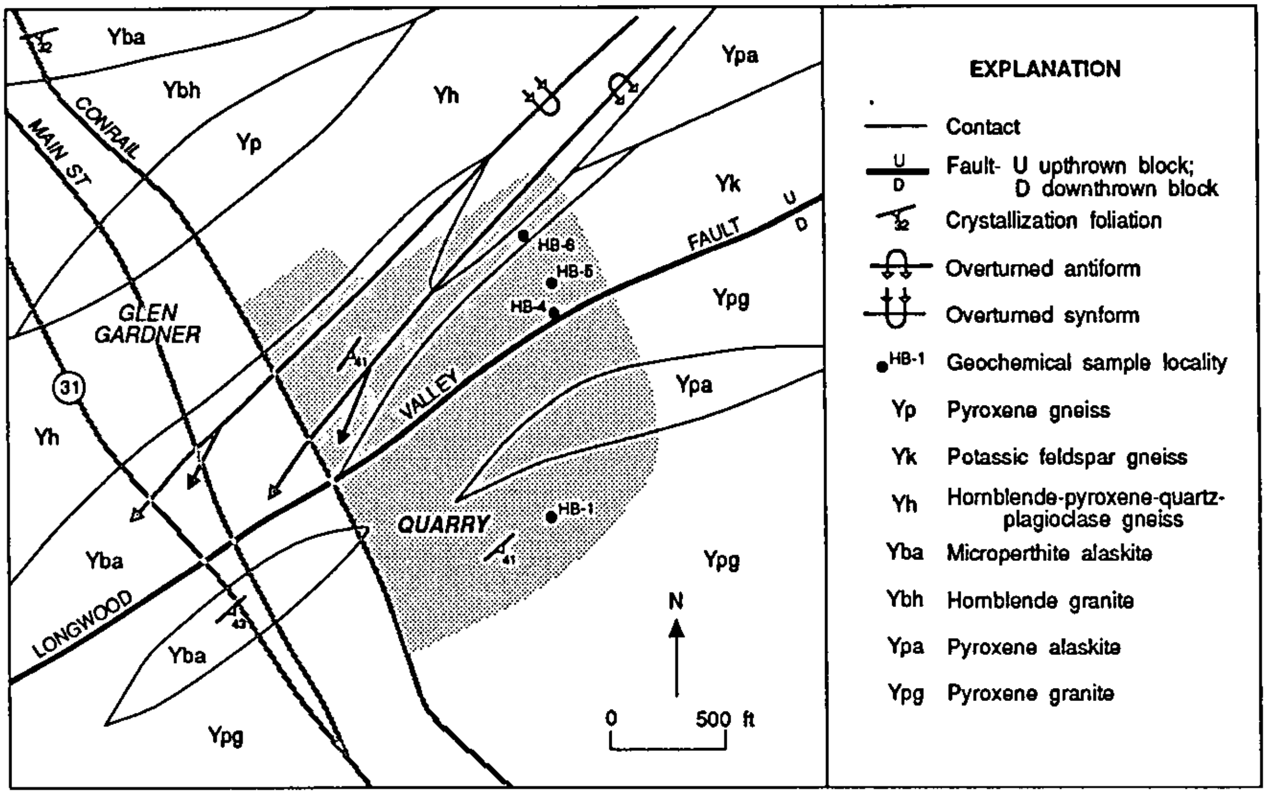

Figure 4 (above). Bedrock geologic map of the Lentine Aggregates quarry, Hunterdon County, New Jersey. Geology from R. Volkert, unpub.

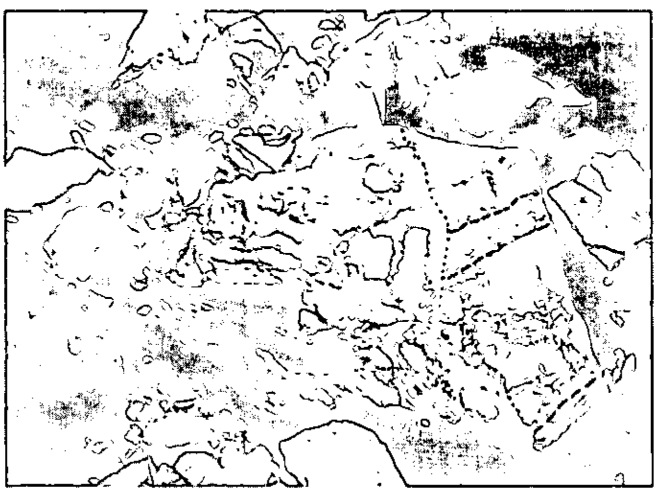

Figure 5 (left). Block showing microperthite alaskite dike (left) in contact (dotted) with and cross cutting foliation (dashed) in hornblende gneiss (right). Lentine Aggregates quarry, Hunterdon County, New Jersey.

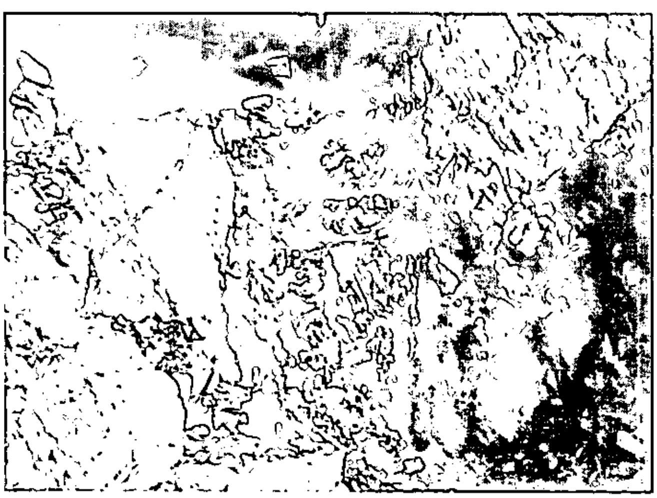

Figure 6 (left). Microperthite alaskite dike (center) cutting hornblende gneiss (right) and hornblende granite (left). Dike contacts are sheared by brittle deformation and altered to epidote and chlorite. Lentine Aggrregates quarry.

quarry. Yet, concentrations of U and Th are not elevated (table 4).

Granites and alaskites in the Highlands are interpreted to be syntectonic and may have crystallized from melt generated by anatexis of crustal material. Some of this material may have been uranium-bearing initially. As a result of magmatic differentiation, this element was concentrated in the residual melt from which alaskites and related pegmatites crystallized. Uranium and thorium have large ionic radii (1.08 angstrom) and high valence charge (+4) preventing them from entering the silicate structures of earlier-formed minerals and concentrating them in late residual fluids (Krauskopf, 1979).

Since shear zones at the quarry typically do not have elevated levels of radioactivity, we suggest that uranium and thorium mineralization occurred during Proterozoic time and that, at least in this locality, these elements were not mobile during subsequent brittle deformation.

29.45	0.4	Backtrack to Rt. 31, turn left onto Sanitorium Rd. Turn right onto Rt. 31 north.
31.55	2.1	Turn left onto Main St.
31.7	1.5	Turn right onto Valley Rd.
32.8	1.1	Crossing Musconetcong River.
32.9	0.1	Turn left onto Maple Ave.
33.2	0.3	Turn left at stop sign onto Rt. 643 south.
33.5	0.3	Bear left onto River Rd.
33.6	0.1	Turn right onto Iron Bridge Rd.
34.0	0.4	STOP 2 (optional) Musconetcong thrust fault along the Central Railroad of New Jersey cut at Iron Bridge Road.

Stop 2 -

In this railroad cut the Musconetcong thrust fault is exposed and brings Middle Proterozoic rocks of the hanging wall into contact with Cambrian dolomite of the Leithsville Formation. This stop illustrates that deformation alone does not remobilize uranium from the crystalline basement into the Paleozoic carbonates. It contrasts with the subsequent stops in the Paleozoic where uranium mineralization has occurred in the carbonates.

The Leithsville is dominantly composed of fine-grained, massive, dark-gray dolomite. Thin shaly and cherty units which occur several meters below the thrust contact are tightly folded. The radioactivity levels measured in the dolomite are very low (40-50 cps).

Three lithologies are present in the Proterozoic hanging wall block of the thrust fault. At the western end of the railroad cut, at the crossing of Iron Bridge Road, the dominant unit is a pyroxene quartzofeldspathic gneiss. Minor shearing and brecciation occur in the gneiss near the thrust contact. The radioactivity measured on the gneiss is relatively low, ranging from 60 to 80-cps. The fault zone itself is not exposed, but the one meter-thick zone of covered slope which separates the Proterozoic from the Paleozoic is also low in radioactivity (60 -70 cps).

Further to the east, along the railroad cut, the hanging wall of the thrust is composed of hornblende granite. This unit is elevated in radionuclides, with average activities measured from 140 to 300 cps and peak values of 1,000 cps. Locally the granite is injected with thin, potassium-feldspar-rich alaskite bodies with average radioactivities of 300 to 600 cps and maximum values up to 2,200 cps. All homes on this alaskite granite lithology measured for radon exceed 4 pCi/l and over 10% of the homes exceed 200 pCi/l.

Along the eastern part of the railroad cut, the trace of the fault and the Leithsville carbonates of the footwall are covered with a talus of radioactive granitic blocks. However, there is no evidence of elevated radioactivity in the fault zone itself or in the carbonates. The dominant control on the distribution of uranium and radon in this area is exerted by the Proterozoic lithologies.

		Backtrack to Rt. 31, turn left onto River Rd., right onto Rt. 643 north, right onto Maple Ave., right onto Valley Rd., left onto Main St. to Rt. 31.
36.45	2.45	Turn right onto Rt. 31 south.
40.55	4.1	Spruce Run Reservoir on right.
41.35	0.8	Turn right into NJ Water Supply Authority facilities and follow driveway around to right. Take gravel road along reservoir to spillway.
43.25	1.9	STOP 3. Spruce Run Reservoir spillway: Lower Paleozoic carbonates with mineralized shear zones

Stop 3 -

Anomalous radioactivity in this area was first recorded through natural gamma aeroradioactivity surveys conducted by the U.S. Geological Survey in the 1960's (Gabelman, 1956; Boynton and others, 1966). The levels observed here were 950 cps with regional background levels of approximately 500-600 cps. With the finding in 1986 of high in-home levels of radon in local housing developments, the entire anomaly was investigated. Both this stop and the next stop (stop 4) at Mulligan's Quarry are within the anomaly. Due to abundant bedrock exposure, they offer a unique opportunity to study the occurrence of elevated radon levels in a carbonate environment. Geological mapping, detailed chemical analysis and scintillometer traverses suggest that the uranium occurrence is secondary in nature and structurally controlled (Gabelman, 1956; Popper and Martin 1982; Kaeding and others, unpublished data, 1987; Henry and others, 1991).

Rocks found at this stop are platform carbonates of Cambrian and Ordovician age (fig. 7). To the east, Middle Proterozoic rocks form the basement on which rest the Lower Cambrian Hardyston quartzite and the Cambrian Leithsville Formation. Stratigraphically higher is the conformable Cambrian Allentown Dolomite which grades upward into the Beekmantown Group of Lower Ordovician age. Regionally, the Beekmantown unconformity separates these older rocks from the overlying Middle Ordovician Jacksonburg Limestone, which crops out just to the west of this stop. To the southeast and west, structurally above this carbonate package are pelites with minor interbedded limestone and graywacke of the Cambrian-Ordovician Jutland sequence, which you will be seeing at Stop 5. Just to the south and west, redbeds and fanglomerates of the Newark Basin unconformably overlie all of the previously mentioned units. It is the Allentown Formation and parts of the Beekmantown Group which will be seen at this stop.

The Allentown Formation and the Beekmantown Group are composed almost entirely of medium- to thick-bedded, light-medium gray to dark-gray, massive to planar laminated, fine- to coarse-grained dolomite. There are locally interbedded dark-gray dolomitic shales, fine quartz sandstone beds and stringers along with lenses and knots of black chert. Rare occurrences of a dark-gray, fine-grained limestone can be found in the middle of the Beekmantown Group. The presence of uranium and the daughter product radon would not be expected in this lithology as a primary occurrence. Chemical analysis supports this and gives background readings for the dolomite and dolomitic shale at 1.4 ppm uranium (25 cps) and 3.9 ppm uranium (50 cps) respectively.

Structurally this rock has undergone multiple deformational events, but the extensional Mesozoic disturbance is the most important when speaking of radon. Two major, high angle cross-strike fault trends, approximately N40°E and N90°E (fig. 8), appear to be the conduits through which the uranium traveled and was concentrated. Not all faults of these trends are mineralized but most of the faults with uranium have these orientations. This faulting created the necessary secondary porosity which allowed the uranium minerals to be precipitated in secondary gouge material and, in the absence of gouge, as a surface coating on discrete fault surfaces. Samples of the fault material yielded 89.4 and 32.5 ppm uranium and 2,100 cps (results from two N40°E trending faults). Preliminary XRD studies suggest that apatite and fluorapatite are the host minerals for the uranium (M. Kaeding, written communication, 1988). Good examples of the min- eralized N40°E trend can be seen on the southeast end of the spillway where the pavement is being eroded away.

A problem which remains unsolved is the original source of the uranium. Several possibilities which are currently under study include Middle Proterozoic granitoid bodies, Ordovician Jutland rocks, and a source associated with the Mesozoic basin. Preliminary data suggest that fluids from pressure solution of the dolomite can be ruled out as a source of the uranium.

45.35	2.1	Backtrack to Rt. 31. Turn right onto Rt. 31 south.
46.35	1.0	Bear right at fork and take Halstead St.
47.05	0.7	Downtown Clinton.
47.15	0.1	Stoplight; turn right onto West Main St. (Rt. 173).
47.35	0.2	Crossing South Branch of Raritan River. Turn right onto Main St.
47.45	0.1	Bear left before bridge into Clinton Historical Museum Center.
47.5	0.05	STOP 4 - Mulligan's Quarry in dolomite of the Kittatinny Supergroup.

Stop 4 -

The occurrence of uranium at this locality was first described in the 1950s (Gabelman, 1956, p. 403). Later work confirmed the presence of the uranium in secondary fault matrix material (Grauch and Zarinski, 1976), but radioactivity was also noted in a "dark cherty to shaly bed measuring about one foot in thickness" (Markewicz, unpub. a). Radon was not considered until 1986, when the housing development above the quarry was found to have elevated levels of radon. Indoor radon levels are characterized by 90% of the homes exceeding 4 pCi/l and 30% of the homes exceeding 200 pCi/l.

The regional geological synthesis for this stop is the same as the Spruce Run Reservoir spillway. The rocks cropping out here are part of the lower section of the Beekmantown Group and are composed dominantly of thin- to medium-bedded, medium- to dark-gray, massive to planar laminated, fine- to medium-grained dolomite with few thin quartz sand stringers, black chert layers and dark-gray dolomitic shale interbeds. Faulting related to Mesozoic extension is evident in the quarry as shown by several smaller slip surfaces and a larger fault, showing several feet of fault gouge, seen on the southern end of the quarry (fig. 9). The faults, which trend in the N40°E and N90°E range, are the carriers of the secondary uranium mineralization. Popper and Martin (1982) studied the open fault on the south end of the quarry and recorded 414 and 249 ppm uranium from the fault breccia. They identified apatite and hydroxyapatite as the uranium-bearing minerals. Recent studies by Kaeding and Henry (written communication, 1988, Henry and others, 1991) support these findings with chemical and mineralogical analyses (table 5). Both studies propose that the uranium came through the fractured rock associated with the faults and precipitated in the matrix material. The presence of the uranium mineralization in the matrix material is clearly shown on radiographs of sections of dolomite core taken from the housing development above the quarry (fig. 10). Uranium-bearing fluids apparently migrated into the fractured dolomite beds adjacent to the faults.

TABLE 5.
GEOCHEMICAL ANALYSIS OF URANIUM FOR SELECT FAULT TRENDS IN MULLIGAN'S QUARRY, CLINTON, NEW JERSEY

	Fault Trend		
	N40°E	N90°E	Background
U ppm (range)	19.1 - 1440	58-767	1.0 - 3.9
U ppm (avg.)	86.7	368	2.2
samples analyzed	5	7	5

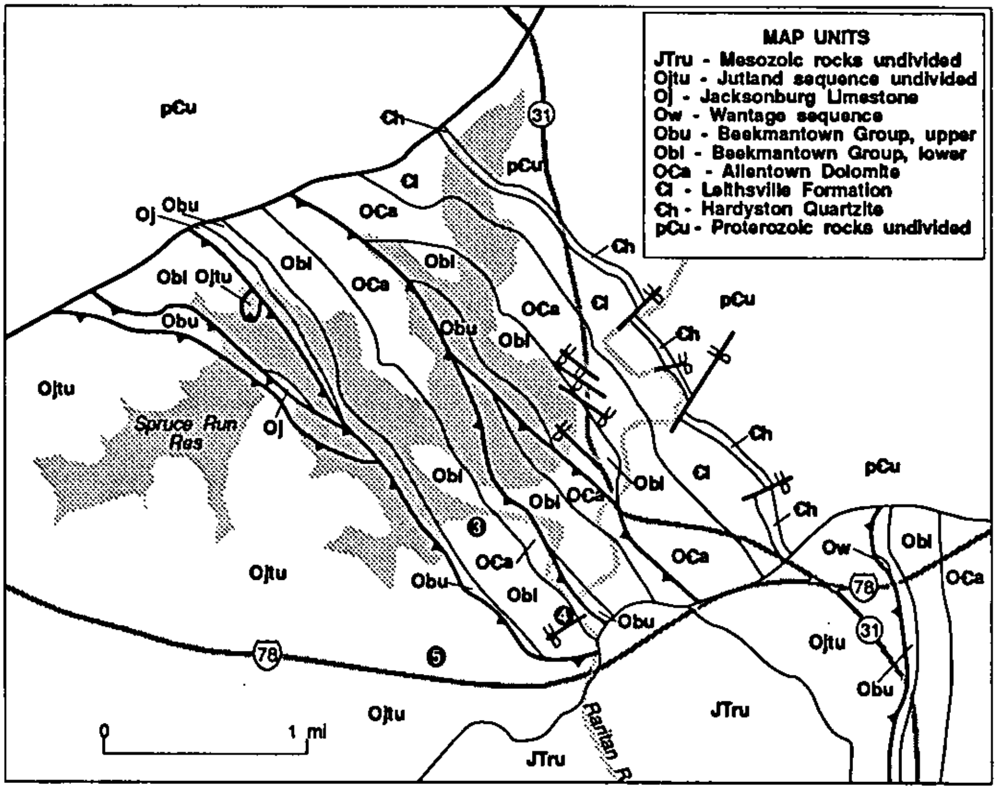

Figure 7. Bedrock geologic map of the Spruce Run Reservoir area, Hunterdon County. Numbers in black circles indicate field stops. Geology from Monteverde, unpub.

Figure 8 (above). Fault zone trending N90°E in Spruce Run Reservoir. Fault gouge is cemented with quartz and uranium-rich apatite.

Figure 9 (right). Gouge zone in a fault trending N40°E at the southern end of Mulligans quarry. This fault is not mineralized. Adjacent uranium-rich faults are responsible for high radon levels in homes.

Recent work on conodonts shows that the conodont alteration index can be used as a thermal index for possible hydrothermal alteration, along with regional and contact metamorphism (Rejebian and others, 1987). Using this technique on several samples collected from the quarry, a higher level of heating was found than the regional one seen in the carbonates elsewhere. Although a limited number of conodonts were found, results suggest that the rocks associated with the uranium mineralization were subjected to hydrothermal mineralizing fluids (J. Repetski, written communication, 1988). Chemical analysis of the fault breccias and the surrounding rocks show positive correlations between uranium concentrations and rare earth elements, thorium, and phosphorous (fig. 11). Preliminary interpretation of rare earth element patterns (not shown) suggests that the dolomite cannot be the source for the uranium.

47.6	0.1	Return to Rt. 173 (Main St.) and turn right.
48.0	0.4	Stoplight; turn right and follow signs for Rt.173.
48.7	0.7	Merge onto I-78 west.
49.1	0.4	Take EXIT 13; bear left and continue on Rt. 173.
50.5	1.4	STOP 5 - Abandoned road metal quarry in Jutland sequence.

Stop 5 -
This stop is located southwest of the town of Clinton in the center of a block of Ordovician clastic and minor carbonate rock termed the Jutland Klippe. The klippe is fault bounded to the northwest by middle Proterozoic rocks; the northeast contact with the Cambrian and Ordovician carbonates is poorly exposed. The Jutland rocks are unconformably overlain by Triassic sediments of the Newark Basin to the south. The age, origin and tectonic setting of the Jutland sequence is controversial (Perissoratis and others, 1979; Markewicz, unpub. a).

A wide range of rock types is found within the Jutland sequence, including varicolored shales, siltstones, sandstones, limestones and cherts. Dark gray, red and brown siltstones and shale are the dominant lithologies at this field stop. However, thin layers of buff-colored and limonite-stained shales are also present. The highest levels of radioactivity (120 cps) are associated with these thin and extremely friable units. The normal background radioactivity for the red and brown shales is about 70 to 80 cps.

A cluster of homes with elevated indoor radon occurs approximately one kilometer south of the field stop in a slightly different part of the Jutland. Here the red shales are less abundant and micritic limestone layers are found. During the construction of a gas pipeline in 1988, the limestone units were well exposed in a trench near the homes with the elevated radon. Background radioactivity for the red and brown shale lithologies in the trench ranged from 120 to 150 cps. Elevated activities (270-500 cps) were measured in association with the limestones and adjacent black shales. Thin layers and veins of a sponge-like, manganese-rich, limonite-stained lithology were also noted within the limestones and shales. These are interpreted as deeply weathered carbonate-sulfide-quartz veins. C horizons of soil immediately overlying these layers were found to contain 48 ppm uranium.

50.6	0.1	Turn left off Rt. 173 and cross over I-78.
50.7	0.1	Turn left and take I-78 east.
53.6	2.9	EXIT 17; take Rt. 31 south.
56.2	2.6	Crossing Flemington fault zone; we are now driving over rocks of the Newark Basin.
57.2	1.0	Small outcrop of Triassic Stockton sandstone on right.
62.6	5.4	Small outcrop of Passaic Fm. on left. Red siltstone dips steeply westward within the Flemington fault zone.
63.7	1.1	Bear right at circle and take Rt. 12 west.
65.2	1.5	Outcrop of gently dipping Lockatong Fm. on right.
66.5	1.3	More outcrops of Lockatong Fm. on both sides of road.
74.2	7.7	Outcrop of Passaic Fm. on left.
75.5	1.3	More outcrops of Passaic Fm. on right.
76.0	0.5	Turn left onto Race St. (Rt. 12 west) in Frenchtown.
76.1	0.1	Turn left onto Trenton Ave. (Rt. 29) and continue south along Delaware River.
80.1	4.0	Passing Warford Creek on left; a thick gray lake-bed sequence in the lower Passaic Fm. is exposed in creek bed. Fine sandstone at base of unit has about 10 times background radioactivity.
80.3	0.2	Continuous outcrops of lowermost Passaic and uppermost Lockatong Fms. begin on left.
81.0	0.7	Contact between Passaic and underlying Lockatong Fm. on left.
81.5	0.5	Outcrop of Lockatong Fm. on left and continuing for next mile.
83.0	1.5	Abandoned quarry in Lockatong Fm. on left.
83.2	0.2	STOP 6 - Lake bed cycles in upper middle Lockatong Fm.

Stop 6 -
Rocks at this stop are cyclically-bedded gray to black siltstone, sandstone, and mudstone of Late Triassic lakes and lake margins. Cycles record transgression, lake highstand, and regression. Transgressive and regressive sequences are lithologically similar, with thick to massive bedding. The fissile lake-bottom beds are the most apparent feature at outcrop scale.

Radioactivity anomalies can occur almost anywhere in a cycle, but are most common in fissile mudstone of lake highstands and in fine sandstone directly below or above fissile beds. Anomalies almost never occur in the upper part of the regressive phase of a cycle.

Nine cycles are exposed here between the fault contact with diabase to the south and an old quarry excavation to the north. Two of the cycles have particularly elevated radioactivity. The third cycle above the diabase has a thin, weakly developed fissile interval (fig. 12). Above the fissile bed, fine sandstone has radioactivity above 1100 cps, more than 10 times typical background level for the Lockatong Formation.

The last cycle before the quarry has a laminated interval about 1m thick; the lower part is covered with rubble. The upper part of the fissile black mudstone unit has radioactivity to 850 cps. The lower part of the overlying thick-bedded siltstone is also moderately hot, with readings ranging from 500 to 180 cps going upward in the unit (fig. 13)

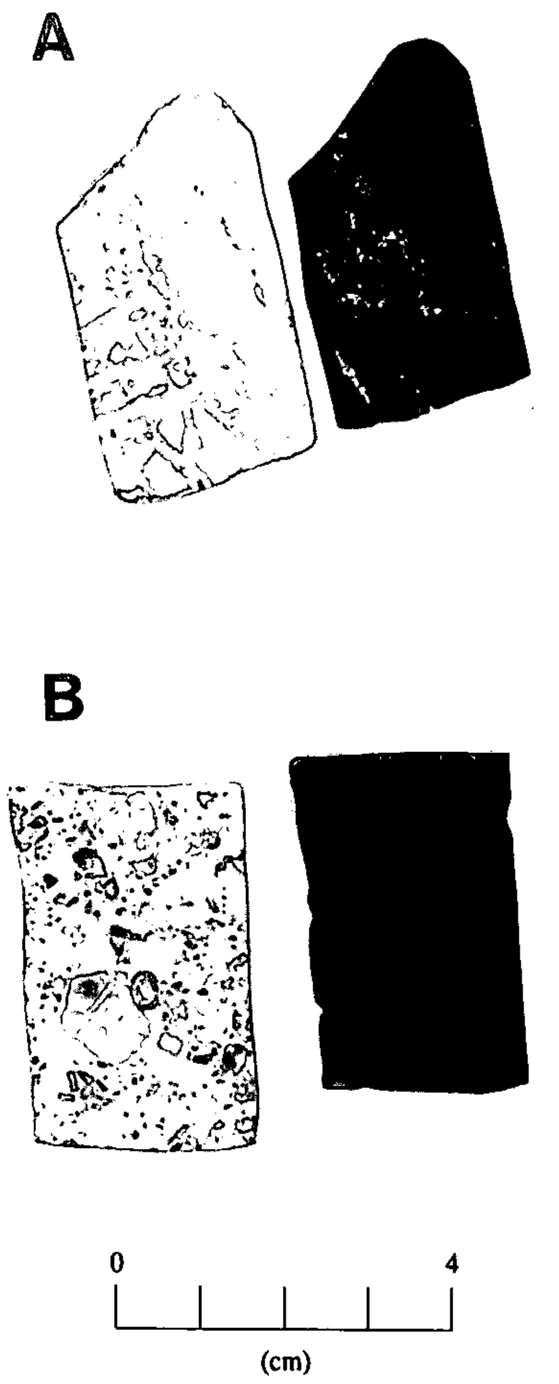

Figure 10 (above). Photographs and autoradiographs of drill core from the Mulligans quarry area showing concentration of uranium mineralization in a) secondary minerals in veinlets in dolomite, and b) cement of massive breccia.

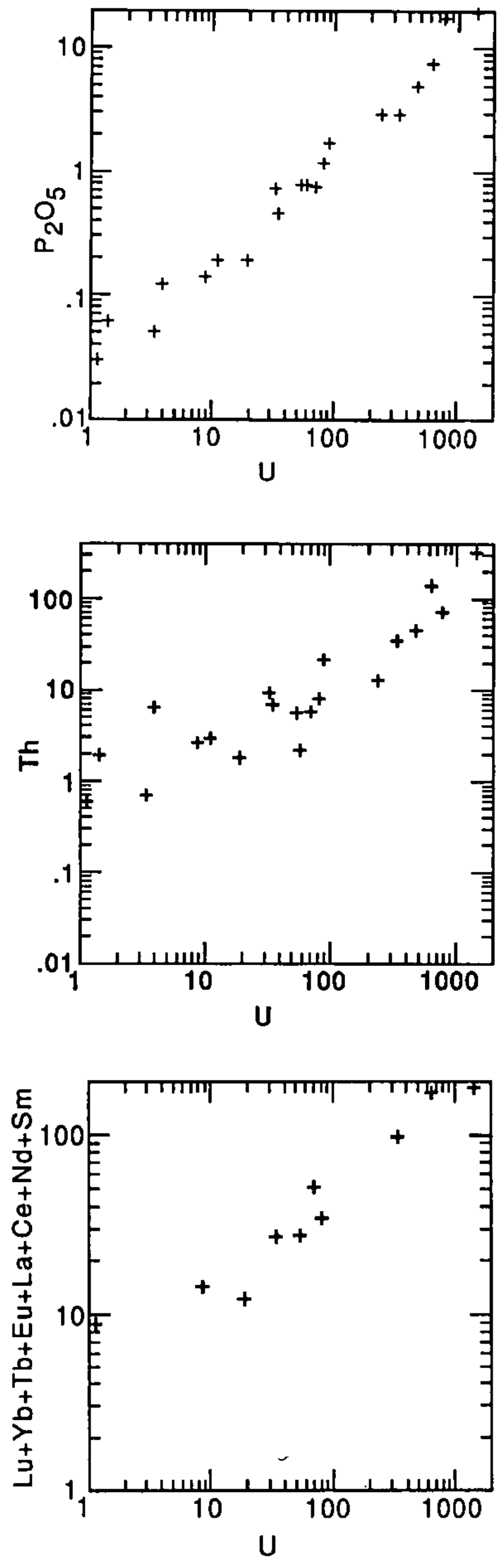

Figure 11 (right). Covariation diagrams showing the correlation of phosphate (P_2O_5), thorium (Th) and rare earth elements (Lu, Yb, Tb, Eu, La, Ce, Nd, and Sm) with uranium (U). P_2O_5 in percent, other elements in parts per million.

83.2	0.0	Continue south on Rt. 29.
83.3	0.1	Jurassic diabase body with faulted upper contact and intrusive lower contact.
84.7	1.4	Outcrop of Stockton Fm. on left.
84.9	0.2	Raven Rock quarry in Stockton Fm. on left; site of uranium ore scam in 1956 (newspaper articles on file at NJGS).
87.3	2.4	Abandoned quarries in Stockton sandstone on left.
88.2	0.9	Town of Stockton.
88.6	0.4	Conglomeratic Stockton Fm. on left.
89.3	0.7	Crossing Flemington fault. Lockatong Fm. and Jurassic diabase on left. Delaware and Raritan Canal on right.
89.7	0.4	Diabase quarry on left. Outcrop at entrance is highly sheared argillite.
90.1	0.4	Crossing Dilts Corner fault, a splay of the Flemington system.
90.6	0.5	Turn right onto cloverleaf ramp to Rt. 202 north.
91.1	0.5	Outcrop of Passaic Fm. on right.
92.0	0.9	Outcrops of Passaic Fm., both sides of road.
92.7	0.7	Outcrops of Passaic Fm.
96.0	3.3	Turn right and take Rt. 31 south.
98.9	2.9	Turn right onto Rt. 612 (Woodsville Rd.).
100.35	1.45	Turn left onto Skyview Dr. and park.
100.35	0.0	STOP 7. Lake bed cycles and red beds in lower Lockatong Fm.

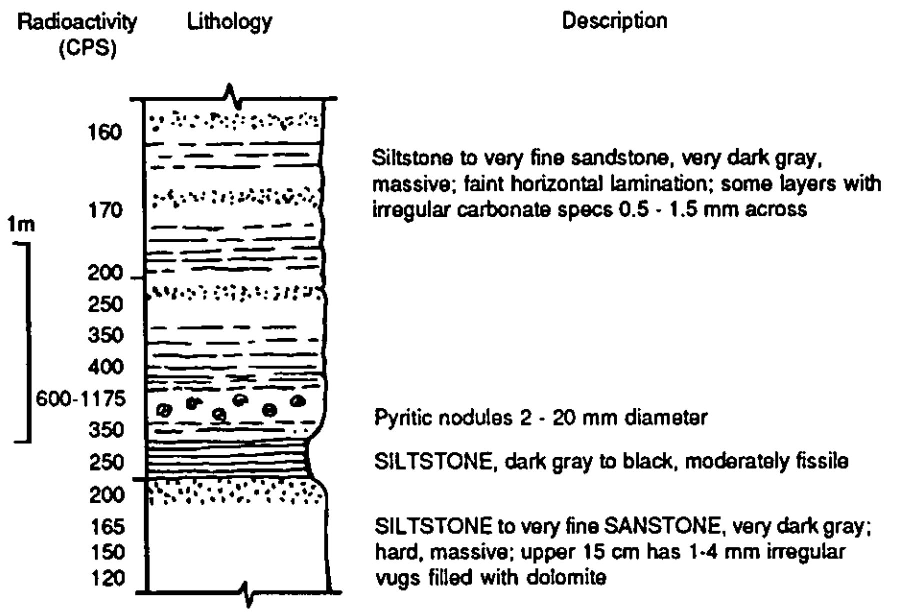

Figure 12. Measured sections of third well-exposed lake cycle above Byram diabase intrusion. Radioactivity in counts per second (CPS).

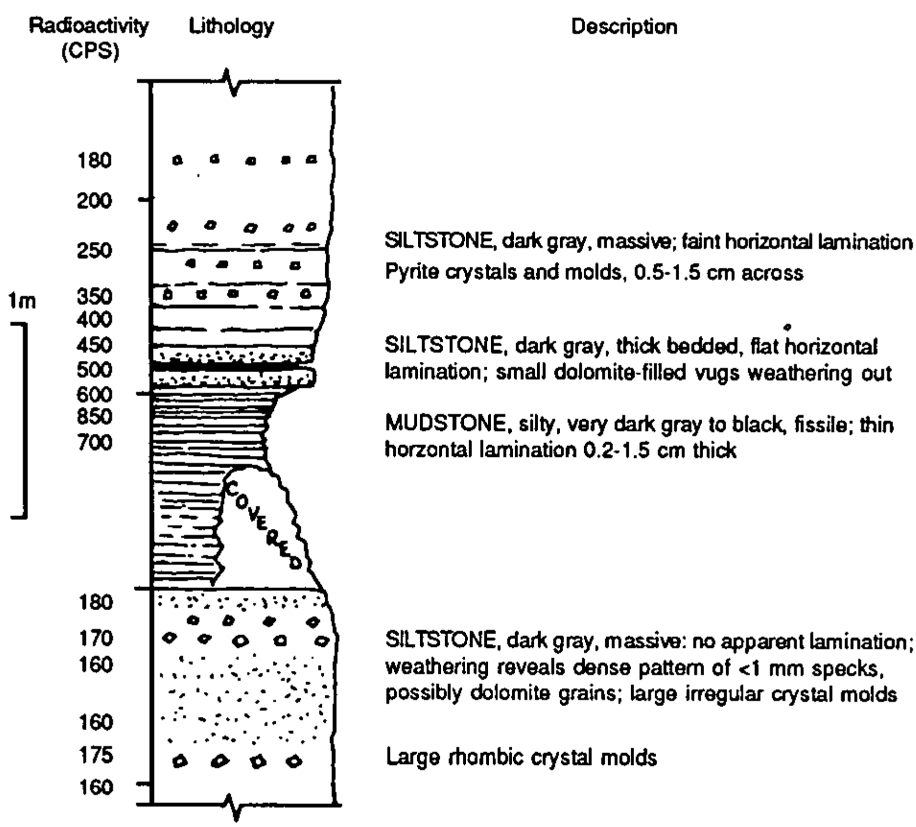

Figure 13. Measured section of uppermost lake cycle south of abandoned quarry, east side of N.J. Rt. 29 at Byram.

Stop 7 -
This roadcut exposes a series of three gray lake-bed cycles bounded below and above by red beds. The red-to-gray transition at the base of these units clearly reveals lithologic changes within thick-bedded siltstone below laminated lake-bottom beds (fig. 14). The color change results from preservation of organic matter, mostly algal (E.I. Robbins, written communication, 1984), in the gray beds. The organic matter prevented oxidation of iron oxides to form hematite and goethite coatings on quartz grains and clay particles. In addition, organic carbon in lake-margin and lake bottom sediments served as reducing medium for immobilizing dissolved U/Th oxides which circulated in ground water and formation water during diagenesis. As at the previous stop, well-developed lake-bed sequences here are short cycles described by Van Houten (1962) as being deposited under cyclically varying climatic conditions. The climate variation is thought to correspond to the quasi-periodic interval of precession of the earth's axis of 19,000 and 23,000 years (Van Houten, 1962; Hays and others, 1976; Olsen, 1986). A series of radioactivity peaks can be observed in the lower two lake cycles. Three of the four peaks above 300 cps occur in thick-bedded siltstone of transgressive stages; one high reading occurs in the lake-bottom stage of cycle 2.

100.35	0.0	Turn left and continue south on Rt. 612.
101.9	1.55	Intersection of Rt. 612 and Rt. 31. Turn right for destinations south and west (Rts. I-95 south and I-295 north). Turn left for destinations north and east (Rts. 202 and I-78).

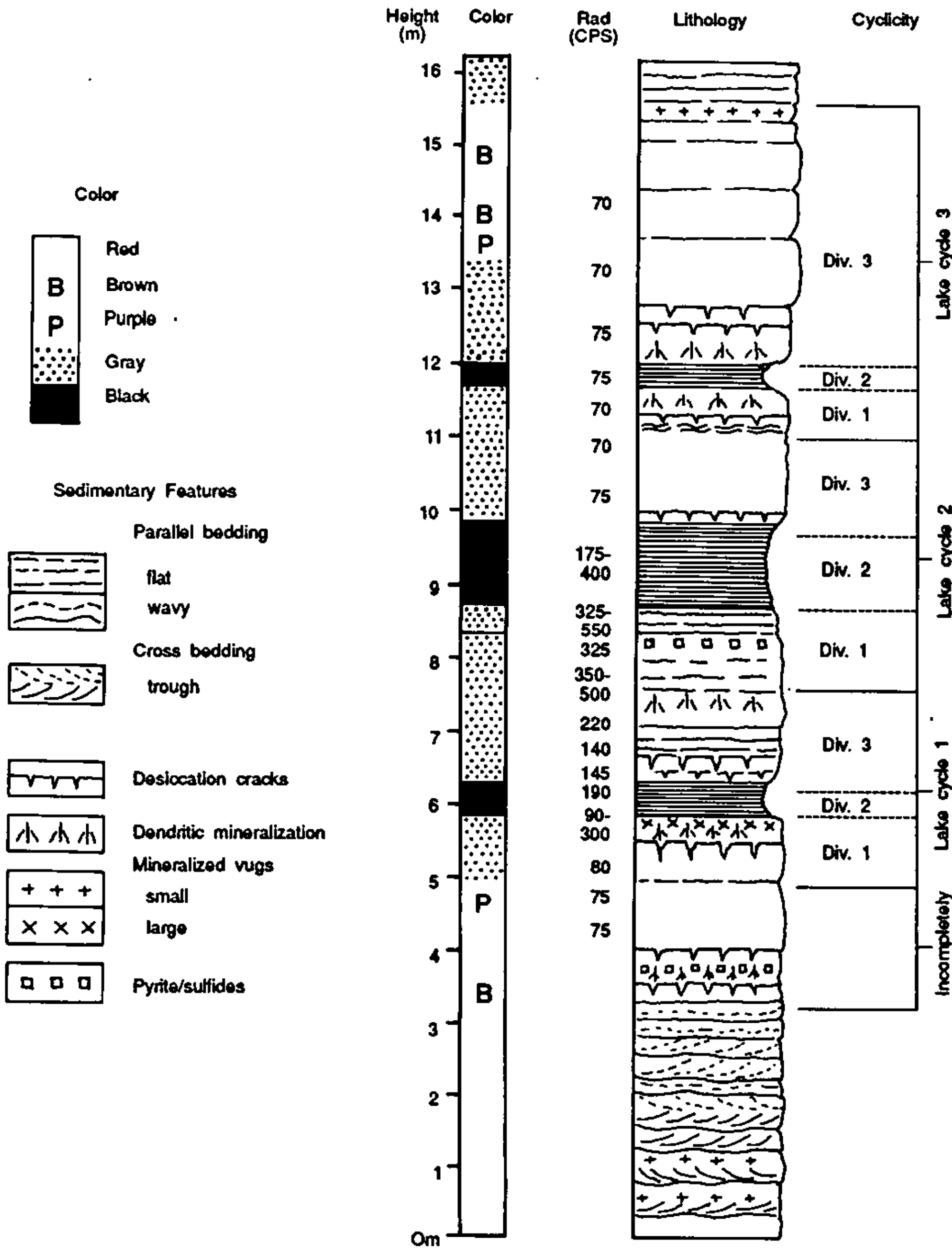

FIELD GUIDE TO THE GEOLOGY OF RADON HAZARD AREAS IN NEW JERSEY
(New Jersey Geological Survey Open-File Report OFR 92-2)